

CHAPTER 144

PREDICTION OF WAVE RUNUP AND RIPRAP STABILITY

By Nobuhisa Kobayashi¹, M.ASCE and Jeffrey H. Greenwald², A.M.ASCE

ABSTRACT: A numerical model has been developed to predict the wave motion on a rough impermeable slope and the hydraulic stability and sliding motion of armor units under the action of a specified normally-incident wave train. The developed numerical model has been compared with riprap test results to calibrate and verify the model.

INTRODUCTION

The present design practices of coastal structures protected with armor units such as breakwaters and revetments are based on hydraulic model tests and empirical formulas although our quantitative understanding of the problem has been improving steadily (4,23,26,29,30). Further improvements of the present design practices will require reliable numerical models which can complement hydraulic model tests since large-scale model tests with minimum scale effects are expensive and time-consuming. Furthermore, some of the important quantities such as the spatial variation of the stability of armor units are very difficult to measure in detail.

As a first attempt, Kobayashi and Jacobs (8) developed a simple analytical model to predict the flow characteristics in the downrush of regular waves on a uniform slope and the critical condition for initiation of movement of armor units. This simple model gives a physical insight into the mechanics of armor stability under the action of surging breakers but is not reliable enough to be applied to actual design problems.

In order to improve the analytical model, Kobayashi et al. (12,13, 14) have developed a numerical model to predict the flow characteristics in the uprush and downrush on a rough impermeable slope and the resulting hydraulic stability and sliding motion of armor units under the action of a normally-incident wave train. Comparison with available riprap test data (1,10) has indicated that the numerical model can predict wave runup, rundown and reflection as well as zero-damage wave heights for uniform and composite riprap slopes if some of the input parameters required for the numerical model are calibrated.

In order to calibrate and verify the developed numerical model more

¹Assoc. Prof., Dept. of Civil Engrg., Univ. of Delaware, Newark, DE 19716.

²Grad. Student, Dept. of Civil Engrg., Univ. of Delaware, Newark, DE 19716; presently, Research Staff, Center of Naval Analysis, Alexandria, VA 22302.

extensively, Kobayashi and Greenwald (15) have conducted eight test runs in a wave tank using a 1:3 glued gravel slope with an impermeable base. For each run with the specified incident wave train generated in a burst, measurements have been made of the free surface oscillation at the toe of the slope, the waterline oscillation on the slope, the temporal variations of dynamic pressures on the base of the slope and the displacements of loose gravel units placed on the glued gravel slope. The calibrated numerical model has been shown to be capable of predicting the measured temporal variations of the hydrodynamic quantities and the measured spatial variations of the amount of the riprap movement.

In this paper the mathematical and numerical backgrounds of the numerical model developed by Kobayashi et al. (12,13,14) are critically reviewed to indicate possible future improvements of the numerical model. Then, the riprap experiment conducted for calibrating and verifying the numerical model is described together with the test results which have not been presented by Kobayashi and Greenwald (15). Furthermore, additional experiments required for further calibration and verification of the numerical model are discussed in light of the limitations of the experiment conducted by Kobayashi and Greenwald (15).

WAVE MOTION ON A ROUGH SLOPE

Wave uprush and downrush on the seaward slope of a coastal structure protected with armor units are similar to wave motions in the swash zone on a beach although the structural slope is normally steeper than the beach slope. It is noted that the surf similarity parameter (3) is widely used to describe the gross wave characteristics on the structural and beach slopes. Use may hence be made of the hydrodynamic models developed for breaking waves on beaches which have been investigated more extensively as reviewed by Peregrine (21). The finite-amplitude shallow-water equations including the effects of bottom friction are suited for predicting the movement of the waterline on the rough slope of the coastal structure if the slope is relatively mild and impermeable. The waterline movement on the slope determines wave runup and rundown and affects the hydraulic stability of armor units as shown by the simple analytical model developed by Kobayashi et al. (8,11). However, the finite-amplitude, shallow-water equations based on the assumption of hydrostatic pressure are not capable of describing detailed two-dimensional behavior of overturning waves (17).

Limiting to the case of a normally-incident wave train on the rough impermeable slope shown in Fig. 1, the finite-amplitude, shallow-water equations including the effects of bottom friction may be written as

$$\frac{\partial h'}{\partial t'} + \frac{\partial}{\partial x'} (h'u') = 0 \quad (1)$$

$$\frac{\partial}{\partial t'} (h'u') + \frac{\partial}{\partial x'} (h'u'^2) = -gh' \frac{\partial \eta'}{\partial x'} - \frac{\tau'_b}{\rho} \quad (2)$$

in which t' = time, x' = horizontal coordinate at the still water level (SWL) which is taken to be positive in the landward direction

with $x' = 0$ at the toe of the slope, $h' =$ water depth below the free surface, $u' =$ depth-averaged horizontal velocity, $g =$ gravitational acceleration, $\eta' =$ vertical displacement of the free surface relative to SWL, $\tau'_b =$ bottom shear stress, and $\rho =$ fluid density which is assumed constant neglecting the effects of air entrainment (5). The bottom shear stress may be expressed as

$$\tau'_b = \frac{1}{2} \rho f' |u'|u' \tag{3}$$

where $f' =$ friction factor associated with the rough impermeable slope which is simply assumed constant. It should be noted that f' will depend on h' if Manning formula is used to express τ'_b (18,19). The empirical formula proposed by Madsen and White (16) has been found satisfactory in estimating the constant value of f' for riprap slopes although additional calibration may be required (13,15).

If the permeability of the underlayer below armor units is not negligible, the flow over the rough permeable bottom and the flow in the permeable underlayer are coupled through the mass and momentum fluxes between these two flow regions. Kobayashi (11) formulated this coupled problem and performed an order-of-magnitude analysis to evaluate the degree of the effects of the permeable underlayer. On the other hand, Hannoura et al. (5) analyzed the flow inside a permeable breakwater using the measured pressure on the rough permeable slope as input. Because of the assumption of the impermeable underlayer, the present numerical model is not applicable to permeable breakwaters such as reef type breakwaters (2).

Denoting the characteristic period and height associated with the normally-incident wave train by T' and H' , respectively, the following dimensionless variables are introduced

$$t = \frac{t'}{T'} \quad , \quad x = \frac{x'}{T' \sqrt{gH'}} \quad , \quad u = \frac{u'}{\sqrt{gH'}} \tag{4}$$

$$z = \frac{z'}{H'} \quad , \quad h = \frac{h'}{H'} \quad , \quad \eta = \frac{\eta'}{H'} \quad , \quad d_t = \frac{d'_t}{H'} \tag{5}$$

in which $z' =$ vertical coordinate which is taken to be positive upward with $z' = 0$ at SWL as shown in Fig. 1, and $d'_t =$ water depth below SWL where the incident wave train may be specified conveniently. Limiting to the case where the incident wave train is well-behaved without any

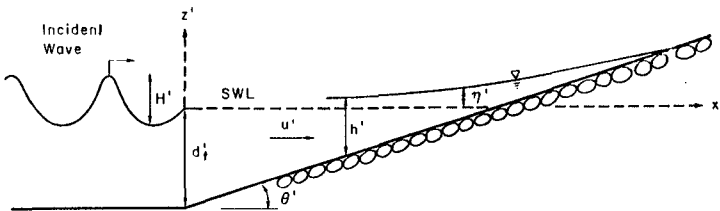


Fig. 1 - Normally-Incident Wave Train on Rough Slope

breaking at the toe of the slope, d'_t is taken to be the water depth below SWL at the toe of the slope as shown in Fig. 1. Substitution of Eqs. 3-5 into Eqs. 1 and 2 yields

$$\frac{\partial h}{\partial t} + \frac{\partial}{\partial x} (hu) = 0 \quad (6)$$

$$\frac{\partial}{\partial t} (hu) + \frac{\partial}{\partial x} (hu^2 + \frac{h^2}{2}) = -\theta h - f|u|u \quad (7)$$

with

$$f = \frac{1}{2} \sigma f' \quad , \quad \sigma = T' \sqrt{\frac{g}{H'}} \quad (8)$$

$$\theta = \sqrt{2\pi} \xi \quad , \quad \xi = \frac{1}{\sqrt{2\pi}} \sigma \tan \theta' \quad (9)$$

in which f = normalized friction factor, σ = dimensionless parameter related to wave steepness, θ = normalized gradient of the slope, and ξ = local surf similarity parameter with θ' = local angle of the slope. For the regular wave incident on a uniform slope of constant θ' as shown in Fig. 1, ξ defined in Eq. 9 reduces to the surf similarity parameter introduced by Battjes (3). The numerical model can easily be applied to examine the effects of the slope geometry on wave runup and armor stability by varying the local slope angle θ' along the slope. Composite slopes approximating the characteristic S-geometry of matured breakwaters have been shown to increase armor stability and reduce wave runup as compared to uniform slopes (4,9,10).

Eqs. 6 and 7 are solved numerically in the time domain to compute h and u as a function of t and x for given θ (i.e., ξ), f , initial and boundary conditions. The initial conditions for h and u are taken such that h = normalized depth below SWL (i.e., $\eta=0$) and $u=0$ at $t=0$ for the region $x \geq 0$ on the rough slope, corresponding to the conditions before the arrival of the incident wave train at the toe of the slope. In general, the computation in the time domain can incorporate nonlinear effects easily relative to the computation in the frequency domain. However, for the incident regular wave train, the time-domain computation starting from the assumed initial conditions at $t=0$ needs to be continued until the state of periodicity is reached. For the computation made by Kobayashi et al. (12,13,14) the transient duration has been limited to the relatively short duration $0 \leq t \leq 5$ where the normalized period of the incident regular wave train is unity. Furthermore, the time-domain computation will become expensive if the number of individual waves in an incident irregular wave train becomes large.

The landward boundary on the rough slope is located at the moving waterline where the water depth h is essentially zero, assuming that no wave overtopping occurs. However, it is desirable to generalize this boundary condition so as to allow wave overtopping over the specified crest geometry of the structure since some wave overtopping is normally accepted in designing the crest geometry (29). If wave overtopping is to be allowed, it will be necessary to apply a discharge relationship at the point of overflow by assuming the similarity between wave overtopping over the crest of the coastal structure and overflow over

a weir in open channel flow (18).

At the seaward boundary located at $x=0$ it is normally required for practical applications to specify the incident waves as input and estimate the reflected waves originating from the region $x \geq 0$ on the rough slope. This implicitly assumes that the reflected waves will not modify the specified incident waves. In order to derive an appropriate seaward boundary condition, Eqs. 6 and 7 are expressed in the corresponding characteristic forms (13). Then, the equation for the seaward-advancing characteristics originating from the region $x \geq 0$ is used to obtain a relationship for the values of u and h at $x=0$. Since an additional relationship is required to find u and h at $x=0$, the normalized total water depth at the seaward boundary is expressed as

$$h = d_t + \eta_i(t) + \eta_r(t) \quad \text{at } x = 0 \quad (10)$$

in which η_i and η_r are the free surface variations normalized by H' at $x=0$ due to the incident and reflected waves, respectively. The superposition of η_i and η_r at $x=0$ implicitly assumes that nonlinear interaction between the incident and reflected waves is negligible in the vicinity of the seaward boundary. The incident wave train at $x=0$ is specified by prescribing the variation of $\eta_i(t)$ with respect to $t \geq 0$. $\eta_r(t)$ may be computed approximately from the value of the seaward advancing characteristic variable at $x=0$ using the relationship between u and η applicable for linear long waves. This approximation is not crucial as long as wave reflection from the rough slope is small and η_r is negligible in Eq. 10. The practical difficulty associated with the seaward boundary condition is that the design incident waves are normally specified in terms of the wave energy spectrum or the significant wave height and period rather than the temporal variation of the free surface associated with the incident wave train which is directly related to the sequence and group of individual waves in an incident irregular wave train. Furthermore, for the incident regular wave train with given H' and T' in the water depth d_t' , $\eta_i(t)$ needs to be estimated using an appropriate wave theory. To specify $\eta_i(t)$ at $x=0$ for given H' , T' and d_t' , Kobayashi et al. (12,13,14) have used cnoidal or Stokes wave theory although these wave theories are not really consistent with the finite-amplitude shallow-water equations. If cnoidal wave theory is applied, it is more consistent to use Boussinesq equations (27). In fact, Pedersen and Gjevik (20) developed a numerical model based on Boussinesq equations for computing runup of a non-breaking solitary wave.

For the specified initial and boundary conditions Eqs. 6 and 7 are solved using an explicit dissipative Lax-Wendroff finite-difference method developed by Peregrine and co-workers (6,7,18,19) for simulating spilling-type breakers and resulting swash oscillations on gentle slopes. In this numerical method, the front of a breaking wave becomes almost vertical without any separate treatment of the wave front but an artificial dissipative term needs to be included to reduce numerical oscillations in the vicinity of the front caused by discretization. Use is made of a finite-difference space and time grid of constant space size Δx and constant time step Δt in which the values of Δx and Δt are determined considering the numerical stability criterion of the

adopted explicit method and the desired spatial and temporal accuracies. Svendsen and Madsen (28) showed that this numerical dissipation would not be required if the effects of turbulence generated by wave breaking were included in the numerical model. Nevertheless, the explicit dissipative Lax-Wendroff finite-difference method has been tested and is relatively easy to apply for simulating the moving waterline on the relatively mild slope where the present computation based on Eqs. 1 and 2 may be appropriate if $(\tan\theta')^2 \ll 1$. The major contribution by Peregrine and co-workers (6,7,18,19) is the development of the predictor-corrector-smoothing procedure dealing with the moving waterline although the details of this procedure are somewhat intuitive and may still be improved (13). As a whole, the adopted numerical method has been found to be very satisfactory although the CPU time for a typical case using 200 nodal points and 2,000 time steps per wave period is approximately 30 sec per wave period (13).

HYDRAULIC STABILITY AND MOVEMENT OF ARMOR UNITS

The finite-difference solution of Eqs. 6 and 7 yields the values of u and h at each of the space grid points along the slope at each time level starting from $t=0$. In order to compute the normalized horizontal water particle acceleration, du/dt , at each space grid point using the computed values of u and h at given time level, Eq. 7 is rewritten as

$$\frac{du}{dt} = \frac{\partial u}{\partial t} + u \frac{\partial u}{\partial x} = - \frac{\partial h}{\partial x} - \theta - \frac{f|u|u}{h} \quad (11)$$

in which use is made of a central-difference approximation of $\partial h/\partial x$. The computed values of u and du/dt at each space grid point at given time level are then used to estimate the hydrodynamic forces acting on an individual armor unit on the rough slope.

The hydraulic stability analysis of stationary armor units performed by Kobayashi et al. (12,14) is similar to the simplified analysis of Kobayashi and Jacobs (8) which was limited to the downrush period only. Fig. 2 shows the forces acting on a stationary armor unit on the $1:\cot\theta'$ slope. Limiting to the case of $(\tan\theta')^2 \ll 1$, it is assumed that the drag force F_D and the inertia force F_I act upward or downward parallel to the slope, whereas the lift force F_L acts upward normal to the slope since the flow tends to be parallel to the slope as shown in Fig. 2. On the other hand, the submerged weight W_S acts

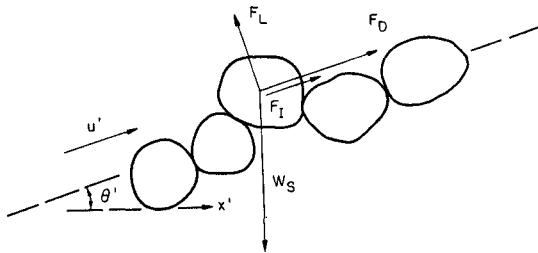


Fig. 2 - Forces Acting on a Stationary Armor Unit

vertically downward. The expressions for F_D , F_I , F_L and W_S are given by Kobayashi and Jacobs (8) except that F_D is proportional to $|u'|u'$ in this analysis for both uprush and downrush periods. The expressions of the hydrodynamic forces F_D , F_I and F_L include the drag, inertia and lift coefficients denoted by C_D , C_M and C_L , respectively. These coefficients need to be determined experimentally on the basis of the simultaneous measurements of the fluid velocity and acceleration and the resulting hydrodynamic forces which will be extremely difficult for an armor unit located on the rough slope under the action of breaking waves. Furthermore, the temporal variations of the hydrodynamic forces can be more complicated than those based on the adopted expressions, judging from the simpler measurements of the lift force on a single sphere near a plane wall in well-behaved oscillatory flow reported by Rosenthal and Sleath (22). Tentatively, Kobayashi et al. (12,14,15) have assumed that for riprap units $C_D = 0.5$, $C_M = 1.5$ and $C_L = 0.18 - 0.4$ in which C_L is varied in this range on the basis of available scattered data on C_L summarized by Sleath (25).

The stability condition for a stationary armor unit against downward or upward sliding or rolling are expressed as

$$|F_D + F_I - W_S \sin\theta'| \leq (W_S \cos\theta' - F_L) \tan\phi \quad (12)$$

in which ϕ = frictional angle of the armor units and $\phi = 50^\circ$ for angular riprap units (8,12,14,15). Limiting to the case of $C_D > (C_L \tan\phi)$, Eq. 12 can be rearranged as

$$N_s = \frac{H'}{s-1} \left(\frac{W'}{\rho g s} \right)^{-1/3} \leq N_R(t, x) \quad (13)$$

where N_s = stability number, s = specific density of the armor unit, W' = weight of the armor unit, ρ = fluid density, and $N_R(t, x)$ = dimensionless function involving u and du/dt which depends on t and x (12,14). Eq. 11 indicates that du/dt may become very large at the wave front where h decreases rapidly with x . The computed fluid accelerations have been found to be as large as $4g$ which may not be unrealistic in comparison with the computed accelerations as large as $5g$ or $6g$ beneath overturning wave crests obtained by New et al. (17). Nevertheless, it has been found necessary to impose the physical bounds, $a_{\min} \leq (du'/dt')/g \leq a_{\max}$, which can be rewritten as

$$a_{\min} \sigma \leq du/dt \leq a_{\max} \sigma \quad (14)$$

in which the values of the dimensionless parameters a_{\min} and a_{\max} are chosen such that Eq. 12 is satisfied for $u=0$ for which $F_D=F_L=0$. The lower bound in Eq. 14 may not be required since the computed values of du/dt have turned out to be greater than $a_{\min} \sigma$ in which $a_{\min} = -0.8$ has been used (14,15). On the other hand, use has been made of $a_{\max} = 1.0$ in the stability computation made by Kobayashi et al. (14,15) on the basis of the experimental results given by Sawaragi et al. (23). This physical upper bound is related to the uncertainty of the computed inertia force using constant C_M at the point of wave breaking as well as to the uncertainty of the response time of an armor unit under the action of the large fluid acceleration of a very short duration.

The stability condition for a stationary armor unit against lifting can be shown to be satisfied as long as Eqs. 13 and 14 are satisfied (14). Consequently, it is sufficient to consider the stability against sliding or rolling for establishing the criterion for initiation of armor movement. For the regular incident wave train specified at $x=0$, it may be sufficient to consider one wave period after the periodicity of the armor stability is established. The local stability number for initiation of armor movement at given location x along the slope is hence defined as

$$N_{sx}(x) = \min[N_R(t,x) | t_p \leq t \leq (t_p + 1)] \quad (15)$$

in which t_p = normalized time when the periodicity of $N_R(t,x)$ with respect to t is established, and the normalized period of the incident wave is unity. Eq. 15 implies that $N_{sx}(x)$ for given x is the minimum value of $N_R(t,x)$ during one wave period after the establishment of the periodicity. The critical stability number N_{sc} for initiation of armor movement is the minimum value of the local stability number $N_{sx}(x)$ which varies along the slope.

The value of the stability number N_s defined in Eq. 13 can be calculated for specified incident wave and armor unit characteristics. The armor units located in the region of $N_s > N_{sx}(x)$ will slide or roll downwards or upwards along the slope. However, the amount of armor movement needs to be predicted to determine whether a specific moving unit will move in place or be dislodged out of place. Wiberg and Smith (31) developed a detailed theoretical model for saltating sediment particles in uni-directional flow. To simplify the analysis for unsteady flow, moving armor units have been assumed to slide essentially parallel to a rough slope without rolling. The displacement X'_a of a sliding armor unit has then been computed by solving the simplified equation of motion for an individual armor unit identified by its initial location on the slope at time $t=0$ (14,15). This computation is based on a Lagrangian approach in which each sliding unit of its representative length d' is followed starting from its initial location at $t=0$ and its subsequent location at each time level is found using the computed normalized displacement $X_a=(X'_a/d')$. As a result, X_a depends on t for each sliding unit identified by its initial location on the slope. The computed normalized displacement may be regarded as a statistical average since the present analysis does not account for the effects of the irregular rough surface on the armor movement explicitly. Moreover, a significant extension of the present analysis will be required to predict the temporal change of the slope profile and the resulting breakwater damage which needs to be considered for the practical design of breakwaters (26). Since the degree of the breakwater damage depends on the wave characteristics during an entire storm such as the number of waves (30), the present numerical model will also need to be simplified to simulate the breakwater behavior during an entire storm.

COMPARISON WITH EXPERIMENTS

Kobayashi et al. (12,13,14) have compared the numerical model with the large-scale riprap tests of Ahrens (1) for uniform slopes with $\cot\theta'=2.5, 3.5$ and 5 in which incident wave trains were generated in a burst and measurements were made of wave runup and zero-damage wave heights. Comparison has also been made with the similar but small-scale riprap tests for composite and 1:3 uniform slopes conducted by Kobayashi and Jacobs (10) who measured wave runup, rundown and zero-damage wave heights. The computed wave runup and rundown using the friction factor $f'=0.3$ have shown to agree with the visually-measured wave runup and rundown. The numerical model with the adopted seaward boundary condition has also predicted the observed increase of the reflection coefficient with the surf similarity parameter (24). Furthermore, the computed critical stability number for initiation of riprap movement has been shown to be in good agreement with the measured zero-damage stability number if the lift coefficient C_L is calibrated in the range $C_L=0.18-0.4$ and the upper bound of the computed fluid acceleration is imposed.

Kobayashi and Greenwald (15) have conducted additional riprap tests in a wave tank which is 36 m long, 2.5 m wide and 1.5 m deep. A piston-type wavemaker controlled by a function generator or a computer is used to generate incident regular wave trains in a burst which are measured using resistance wire wave gages with a wave-absorber beach in the tank. The water depth in the tank is kept constant and $d_t'=0.4$ m in these tests. A 1:3 glued gravel slope with an impermeable base is installed in the tank and exposed to the same incident wave trains. The incident wave conditions considered for eight test runs correspond to plunging, collapsing and surging breakers. For each run with given incident wave train and slope characteristics, measurements are made of the free surface oscillation at the toe of the 1:3 slope, the oscillation of the waterline on the slope, wave pressures on the base of the slope and the displacements of loose gravel units placed on the glued gravel slope. These measured quantities are normalized and compared with the computed normalized quantities for each run. Kobayashi and Greenwald (15) have presented the summary of the comparisons and the detailed results for Runs 2 and 7 which have been selected as typical runs involving plunging and surging breakers, respectively. In the following, the compared results for Run 4 are presented as a typical run for collapsing breakers.

For Run 4 the surf similarity parameter $\xi=3.1$, the normalized water depth at the toe of the slope $d_t'=5.6$ and the dimensionless parameter related to wave steepness $\sigma=24$. Use is made of the friction factor $f'=0.1$ after comparing the measured oscillation of the waterline with the computed results using $f'=0.1$ and 0.2 . Fig. 3 shows the normalized measured oscillation $\eta_i(t)$ for the incident wave train specified as input for the numerical computation. Fig. 3 also shows the computed oscillation $\eta_r(t)$ at the toe of the slope associated with the normalized reflected wave train. Fig. 4 shows the comparison between the measured and computed free surface oscillation $\eta_t(t)$ at the toe of the 1:3 gravel slope in which the computed oscillation $\eta_t(t)$ is the sum of $\eta_i(t)$ and $\eta_r(t)$ shown in Fig. 3. Fig. 4 indicates

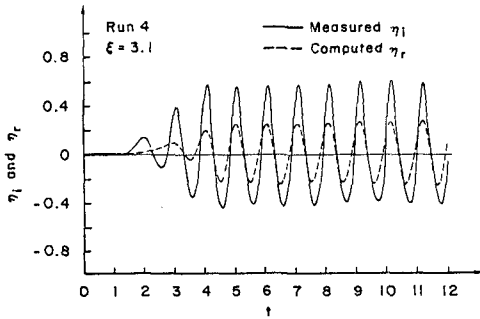


Fig. 3 - Incident and Reflected Wave Trains

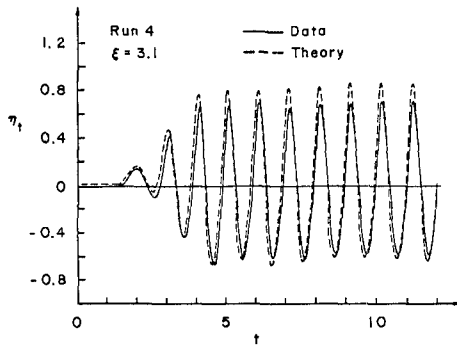


Fig. 4 - Measured and Computed Free Surface Oscillations

appropriateness of the seaward boundary condition used in the numerical model. Fig. 5 shows the comparison of the measured and computed oscillations $z_w(t)$ of the waterline on the 1:3 gravel slope expressed in terms of its vertical elevation relative to SWL normalized by the incident wave height H' . On the other hand, Fig. 6 shows the comparison of the measured and computed dynamic pressure variations at the depth $d'=10$ cm below SWL expressed in terms of $\eta_p(t) = [p' / (\rho g H')]$ with p'_p measured dynamic pressure excluding the hydrostatic pressure below SWL. In summary, the agreements between the measured and computed hydrodynamic quantities are similar to those shown in Figs. 4 and 5 but the agreements for η_p are poor for Runs 3 and 4 corresponding to collapsing breakers. The assumption of hydrostatic pressure used in Eq. 2 may not be appropriate at the particular location of the pressure measurement for Runs 3 and 4.

The additional input parameters required for the computation of the hydraulic stability and movement of armor units have been summarized by Kobayashi and Greenwald (15). The lift coefficient C_L alone has been calibrated by trying $C_L=0.3$ first and then $C_L=0.18$ or 0.4 if necessary. For Run 4 the lift coefficient $C_L=0.3$ and the stability number $N_s=2.2$.

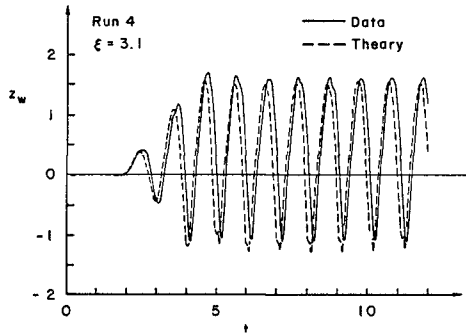


Fig. 5 - Measured and Computed Waterline Oscillations

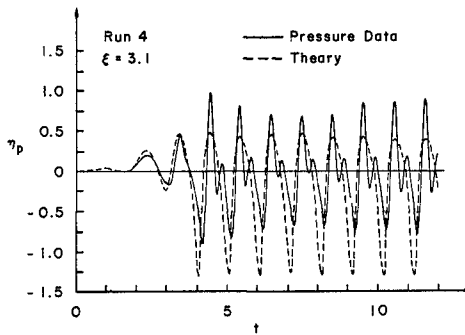


Fig. 6 - Measured and Computed Dynamic Pressure Variations at $d'_p = 10$ cm

Fig. 7 shows the computed variation of the local stability number N_{sx} defined by Eq. 15 as a function of the normalized vertical location z

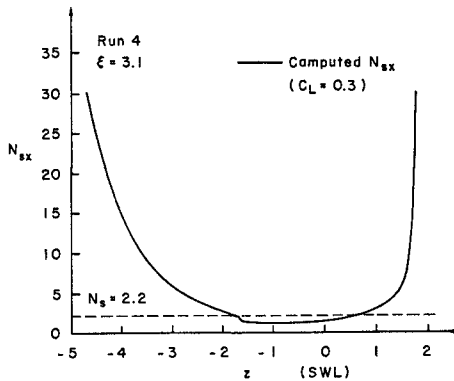


Fig. 7 - Computed Variation of Local Stability Number along 1:3 Slope

relative to SWL along the 1:3 gravel slope. The wave action on the slope is limited in the range $-d_t \leq z \leq R$ where R = computed upper limit reached by the uprushing water above SWL. Loose gravel units placed in the region where $N_S > N_{SX}$ are predicted to move. Fig. 8 shows the comparison between the measured displacements of loose gravel units normalized by the representative length of the units and the computed normalized displacement X_a at the end of the specified incident wave train. The measured and computed values of X_a are plotted as a function of the initial location z on the slope of an individual gravel unit. The negative value of X_a implies the downward movement along the slope. All the measured values of X_a for the eight runs are negative or zero. The data points along the line $X_a=0$ in Fig. 8 correspond to the loose gravel units which are not displaced. On the other hand, the computed points in Fig. 8 include only the displaced units located initially at the finite-difference grid points used for the computation.

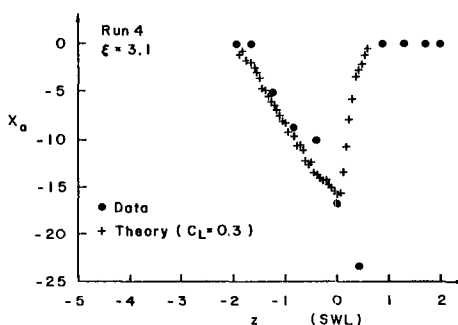


Fig. 8 - Measured and Computed Gravel Unit Displacements

In summary, the agreements between the measured and computed displacements are reasonably good for most of the eight runs.

CONCLUSION

The numerical model developed by Kobayashi et al. (12,13,14) has been shown to be capable of predicting the measured quantities related to the wave motion on the riprap slope and the hydraulic stability and movement of riprap units (1,10,15). However, these measurements limited to the quantities which can be measured fairly easily are not sufficient for determining the friction factor f' and the hydrodynamic coefficients C_L , C_D and C_M in a rigorous manner. The fluid velocities and resulting hydrodynamic forces need to be measured so as to better establish these parameters for different armor units. Furthermore, the numerical model needs to be improved and extended to make it as versatile as hydraulic model testing although the present numerical model yields the quantities of practical importance which are difficult to measure.

ACKNOWLEDGMENT

This study has been supported by the National Science Foundation under Grant No. CEE-8408996.

REFERENCES

1. Ahrens, J.P., "Large Wave Tank Tests of Riprap Stability," Tech. Memo. No. 51, U.S. Army Coastal Engineering Research Center, Ft. Belvoir, Va., 1975.
2. Ahrens, J.P., "Reef Type Breakwaters," Proceedings of 19th Coastal Engineering Conference, ASCE, 1984, pp. 2648-2662.
3. Battjes, J.A., "Surf Similarity," Proceedings of 14th Coastal Engineering Conference, ASCE, 1974, pp. 466-480.
4. Bruun, P., Design and Construction of Mounds for Breakwaters and Coastal Protection, Elsevier, New York, 1985.
5. Hannoura, A.A. and McCorquodale, J.A., "Rubble Mounds: Numerical Modeling of Wave Motion," Journal of Waterway, Port, Coastal and Ocean Engineering, Vol. 111, No. 5, 1985, pp. 800-816.
6. Hibberd, S., "Surf and Run-up," presented to the University of Bristol, at Bristol, U.K., in 1977, in partial fulfillment of the requirements for the Ph.D. degree in Mathematics.
7. Hibberd, S. and Peregrine, D.H., "Surf and Runup on a Beach: A Uniform Bore," Journal of Fluid Mechanics, Vol. 95, Part 2, 1979, pp. 323-345.
8. Kobayashi, N. and Jacobs, B.K., "Riprap Stability Under Wave Action," Journal of Waterway, Port, Coastal and Ocean Engineering, ASCE, Vol. 111, No. 3, 1985, pp. 552-566.
9. Kobayashi, N. and Jacobs, B.K., "Experimental Study on Sandbag Stability and Runup," Proceedings of Coastal Zone '85, ASCE, Vol. 2, pp. 1612-1626
10. Kobayashi, N. and Jacobs, B.K., "Stability of Armor Units on Composite Slopes," Journal of Waterway, Port, Coastal and Ocean Engineering, ASCE, Vol. 111, No. 5, 1985, pp. 880-894.
11. Kobayashi, N., "Closure of Riprap Stability Under Wave Action," Journal of Waterway, Port, Coastal and Ocean Engineering, ASCE, Vol. 112, No. 6, 1986, pp. 673-681.
12. Kobayashi, N., Roy, I. and Otta, A.K., "Numerical Simulation of Wave Runup and Armor Stability," OTC Paper 5088, 18th Offshore Technology Conference, Vol. 1, Houston, Texas, 1986, pp. 51-56.
13. Kobayashi, N., Otta, A.K. and Roy, I., "Wave Reflection and Runup on Rough Slopes," to appear in Journal of Waterway, Port, Coastal and Ocean Engineering, ASCE, Vol. 113, 1987.
14. Kobayashi, N. and Otta, A.K., "Hydraulic Stability Analysis of Armor Units," to appear in Journal of Waterway, Port, Coastal and Ocean Engineering, ASCE, Vol. 113, 1987.
15. Kobayashi, N. and Greenwald, J.H., "Waterline Oscillation and Riprap Movement," submitted to Journal of Waterway, Port, Coastal and Ocean Engineering, ASCE, 1987.
16. Madsen, O.S. and White, S.M., "Energy Dissipation on a Rough Slope," Journal of the Waterways, Harbors and Coastal Engineering Division, ASCE, Vol. 102, No. WW1, 1976, pp. 31-48.
17. New, A.L., McIver, P. and Peregrine, D.H., "Computation of Over-

- turning Waves," Journal of Fluid Mechanics, Vol. 150, 1985, pp. 233-251.
18. Packwood, A.R., "Surf and Run-up on Beaches," presented to the University of Bristol, at Bristol, U.K., in 1980, in partial fulfillment of the requirements for the Ph.D. degree in Mathematics.
 19. Packwood, A.R. and Peregrine, D.H., "Surf and Run-up on Beaches: Models of Viscous Effects," Report No. AM-81-07, School of Mathematics, University of Bristol, Bristol, U.K., 1981.
 20. Pedersen, C. and Cjevik, B., "Runup of Solitary Waves," Journal of Fluid Mechanics, Vol. 135, 1983, pp. 283-299.
 21. Peregrine, D.H., "Breaking Waves on Beaches," Annual Review of Fluid Mechanics, Vol. 15, pp. 149-178.
 22. Rosenthal, C.N. and Sleath, J.F.A., "Measurements of Lift in Oscillatory Flow," Journal of Fluid Mechanics, Vol. 164, 1986, pp. 449-467.
 23. Sawaragi, T., Ryu, C. and Iwata, K., "Considerations of the Destruction Mechanism of Rubble Mound Breakwaters Due to the Resonance Phenomenon," Proceedings of 8th International Harbour Congress, Antwerp, Belgium, 1983, pp. 3.197-3.208.
 24. Seelig, W.N., "Wave Reflection from Coastal Structures," Proceedings of Coastal Structures '83, ASCE, 1983, pp. 961-973.
 25. Sleath, J.F.A., Sea Bed Mechanics, Wiley-Interscience, New York, 1984.
 26. Smith, O.P., "Cost-Effective Optimization of Rubble-Mound Breakwater Cross Sections," Tech. Report CERC-86-2, U.S. Army Coastal Engineering Research Center, Vicksburg, Ms. 1986.
 27. Svendsen, I.A. and Jonsson, I.G., Hydrodynamics of Coastal Regions, Technical University of Denmark, Lyngby, Denmark, 1980.
 28. Svendsen, I.A. and Madsen, P.A., "A Turbulent Bore on a Beach," Journal of Fluid Mechanics, Vol. 148, 1984, pp. 73-96.
 29. U.S. Army Coastal Engineering Research Center, Shore Protection Manual, Vol. II, U.S. Government Printing Office, Washington, D.C., 1984.
 30. Van der Meer, J.W. and Pilarczyk, K.W., "Stability of Rubble Mound Slopes under Random Wave Attack," Proceedings of 19th Coastal Engineering Conference, ASCE, 1984, pp. 2620-2634.
 31. Wiberg, P.L. and Smith, J.D., "A Theoretical Model for Saltating Crains in Water," Journal of Geophysical Research, Vol. 90, No. C4, 1985, pp. 7341-7354.